Oceanologia (2016) 58, 187—195

Available online at www.sciencedirect.com

ScienceDirect

journal homepage: www.elsevier.com/locate/oceano

ORIGINAL RESEARCH ARTICLE

Fisher—Shannon analysis of the time variability of remotely sensed sea surface temperature at the Brazil—Malvinas Confluence☆

Jorge O. Pierini [a], Michele Lovallo [b], Eduardo A. Gómez [c], Luciano Telesca [d,*]

[a] *Comisión de Investigaciones Científicas (CIC)—UCALP-CCT-BB (IADO-CONICET), CC 804, Bahía Blanca, Argentina*
[b] *ARPAB, Potenza, Italy*
[c] *CCT-BB (IADO-CONICET), UTN Facultad Regional Bahía Blanca, Bahía Blanca, Argentina*
[d] *National Research Council, Institute of Methodologies for Environmental Analysis, Tito, PZ, Italy*

Received 8 May 2015; accepted 12 February 2016
Available online 19 March 2016

KEYWORDS
Brazil—Malvinas Confluence Zone;
Fisher—Shannon method;
Ocean

Summary The collision of the warm and salty southward flowing Brazil Current and the cold and relatively fresh northward flowing Malvinas Current produces a strong frontal zone known as the Brazil—Malvinas Confluence Zone (BMCZ). This is featured by intense presence of eddies and meanders and is one of the most energetic areas of the world oceans. We apply the statistical method of Fisher—Shannon (FS) to the time series of sea surface temperature, derived from the satellite Advanced Very High Resolution Radiometer (AVHRR) imagery, acquired from 1984 to 1999. The FS method consists of the joint application of Fisher information measure (FIM) and Shannon entropy (SE), measuring respectively the degree of organization and the disorder of a system. Our findings indicate that the FS method is able to locate very clearly the BMCZ, which corresponds to the less organized and more disordered area within the area of confluence between the Brazil and Malvinas Currents.

☆ The study was supported by the 2014—2016 Bilateral Project Italy-Argentina "Use of satellite technologies for large-scale oceanographic and environmental studies over the Argentinean Continental Shelf' funded by MINCyT and MAECI.
* Corresponding author at: National Research Council, Institute of Methodologies for Environmental Analysis, Tito, PZ, Italy
E-mail address: luciano.telesca@imaa.cnr.it (L. Telesca).
Peer review under the responsibility of Institute of Oceanology of the Polish Academy of Sciences.

ELSEVIER Production and hosting by Elsevier

http://dx.doi.org/10.1016/j.oceano.2016.02.003

1. Introduction

The South Atlantic's circulation presents several characteristics that are very significant for climate variability. In this region, which is the main source of equatorial surface and thermocline waters (Blanke et al., 1999; Matano et al., 1993; Speich et al., 2007), the circulation affects the climate of the surrounding continents by influencing the distribution of the sea surface temperature (SST) through lateral advection and/or by propagation of anomalies within the mixed layer (Kushnir et al., 2002). The South Atlantic is linked with the Indian and Pacific Oceans, and therefore it provides a gateway by which the Atlantic meridional overturns.

In the South Atlantic, the Brazil–Malvinas Confluence Zone (BMCZ) is crucial to understand circulation and heat transport processes (Wainer et al., 2000). The BMCZ is located off the coast of Argentina and Uruguay, at the convergence between the warm poleward flowing of the Brazil Current and the cold equatorward flowing of the Malvinas Current, between 35°S and 45°S latitude and 50°W to 70°W longitude. The confluence of these two currents originates a strong thermocline and the formation of many high energy eddies (Maamaatuaiahutapu et al., 1998) (Fig. 1).

The Brazil Current carries warm subtropical water with typical temperature values between 18 and 28°C. It generally flows in the upper 600 m of the ocean and its volume transport at the confluence zone is upwards of 20 Sv with speeds over a half a meter per second (Evans et al., 1983; Memery et al., 2000; Peterson and Stramma, 1990). The Malvinas Current, a branch off of the Antarctic Circumpolar Current, carries cold and relatively fresh subantarctic water, between 60 and 90 Sv and speeds varying from about 0.5 m s^{-1} to about 1 m s^{-1}. Interestingly, the Malvinas Current extends all the way to the sea-floor, contrarily to the Brazil Current that is a surface current. The temperature ranges typically around 6°C (Vigan et al., 2000; Vivier and Provost, 1999).

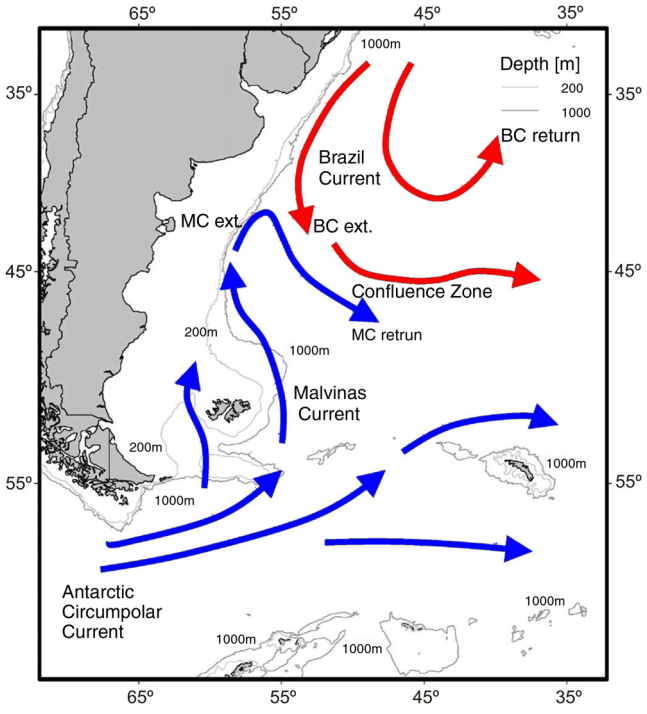

Figure 1 Map of the Argentinean continental shelf with the warm poleward flowing Brazil Current (red) and the cold equatorward flowing Malvinas Current (blue). Also indicated are the Malvinas Current return (MC return), the Brazil Current extension (BC ext.) and the Brazil Current return (BC return). The continent and the shelf up to the 1000 m and 200 m isobath are indicated by dark gray and light gray line respectively. (For interpretation of the references to color in this figure legend, the reader is referred to the web version of this article.)

After the collision with the Malvinas Current at around 38°S, the Brazil Current branches off into two different paths: the first path is redirected back to the equator creating a large anticyclonic eddy with the original Brazil Current; the second one, which is much stronger than the first one deflects about 45°E of its original tract poleward (Maamaatuaiahutapu et al., 1998). On the contrary, after the collision the surface flow for the Malvinas Current becomes much simpler, being redirected poleward, till about 50°S latitude where it once again is detached back up by the Antarctic Circumpolar Current and heads East (Matano, 1993).

The southeast deflected Brazil Current flows just east of the redirected Malvinas current at around 57.5°W and between 40°S and 45°S (Saraceno et al., 2004, 2006). In this region SST gradients can be as high as 1°C per kilometer. In this zone, which is characterized by very high energy among the world oceans (Gordon, 1989), the meanders, eddies, and filaments are extraordinary. The strong mixing processes cause high-speed cooling of subtropical waters conveyed by the Brazil Current, characterizing this area as very important for the circulation and heat transport processes (Wainer et al., 2000). Provost and Le Traon (1993) report the high inhomogeneity and anisotropy of the BMCZ at the mesoscale. At shorter frequencies, the Brazil–Malvinas Confluence variability is intense and is principally governed by the yearly and semi-annual cycles (Fu, 1996). Podesta et al. (1991) show that the yearly periodicity is responsible for the most of the SST variability in the southwestern Atlantic, and, in particular, of more than 80% of the SST variability on the continental shelf off the southwestern Atlantic Ocean. The eddies, extremely energetic, are featured by intense rotational velocity. Eight or nine different mesoscale eddies with many other microscale eddies could exist at any time. Even if many studies have been done on these high energy turbulent mixing areas, the deep knowledge of these mesoscale processes is still challenging and far from being completely understood (Tokinaga et al., 2005).

Joint use of advanced statistical techniques and satellite images have advanced our knowledge of the relevant scales and features of ocean properties (i.e., Denman and Abbott, 1994; Doney et al., 2003; Lentini et al., 2002; McClain et al., 1998; Stammer, 1997). The application of singularity analysis to SST images has recently suggested a different conceptual approach to the identification of flow patterns from satellite images (Isern-Fontanet et al., 2007; Turiel et al., 2005). Experimental studies of the chaotic properties of oceanic processes have been performed for several years; for instance, Osborne et al. (1986) and Brown and Smith (1990, 1991) investigated deeply the chaotic behavior of oceanic large and mesoscale motions.

Up to now, the majority of researches dealing with SST satellite images in the BMCZ have focused on the complexity of the mesoscale surface structures. Podesta et al. (1991) and Legeckis (1978), using National Oceanic and Atmospheric Administration (NOAA) Advanced Very High Resolution Radiometer (AVHRR) imagery, revealed the highly time variability of the southward extension of the Brazil Current and eddy generation.

In our study, we aim at describing quantitatively the temporal variations of the SST in the BMCZ by using a statistical approach, the so called Fisher–Shannon (FS) method, never used in the context of ocean dynamics and in particular to investigate the variability of the SST. The FS approach is based on the information content of the time series using the statistical measures of the Fisher information measure and the Shannon entropy, and is a powerful statistical method to gain into insight the inner dynamics of a complex system like the BMCZ.

2. Data

The SST data analyzed in the present study were part of those produced for the western South Atlantic Ocean on the base of the agreement between Servicio Meteorológico Nacional of Argentina (SMN) and the University of Miami's Rosenstiel School of Marine and Atmospheric Science (RSMAS). The SST fields were derived from data collected by the Advanced Very High Resolution Radiometer (AVHRR), (Olson et al., 1988; Podesta et al., 1991), an infrared radiometer flying onboard polar-orbiting satellites of the National Oceanic and Atmospheric Administration (NOAA). For more information on the AVHRR and NOAA satellites, the reader is referred to the Users' Guide available on www.noaa.gov. The data were recorded at the HRPT Receiving Station operated by SMN in Villa Ortúzar, Buenos Aires, Argentina.

The SST was subjected to atmospheric correction by measuring radiance from the same field of view at two wavelengths (Anding and Kauth, 1970; McClain et al., 1985).

The SST data were compared to in situ measurement for the investigated area (Bava, 2004; Bava et al., 2002; Kilpatrick et al., 2001; Lentini et al., 2001; Saraceno et al., 2004).

The time span is 15 years, from July 1984 to July 1999 and is constituted by 1080 5-day composite images with an approximately 4 km × 4 km resolution. The compositing is done by keeping the warmest pixel among all images available for the 5-day period; in this manner, if a pixel is cloud-contaminated, its temperature is generally lower than that of a pixel in open water. As clouds move within the compositing considered period, the same pixel on a subsequent image may be cloud-free and, consequently, will have a higher SST value. By keeping the warmest value in a series of images, one would decrease the cloud coverage effect in the composited image. However, despite the numbers of individual composite images, cloud coverage would persist over some areas at some times, causing that the SST retrievals for some pixels are not valid in some composite images (Bernstein and Chelton, 1985; Njoku, 1985; Njoku et al., 1985). Fig. 2 shows the spatial distribution of the mean SST value and, as an example, the time variation of five pixels in the BMCZ.

3. The Fisher information measure and the Shannon entropy

The Fisher information measure (FIM) and the Shannon entropy are statistical quantities well known in the context of information theory, efficiently used to investigate complex non-stationary signals. The FIM reveals how much organized or ordered is a time series, while the Shannon entropy informs on how much uncertain or disordered a system is.

The FIM was first introduced by Fisher (1925) in the context of estimation theory. Later, it was employed in large variety of applications. Frieden (1990) employed the FIM to represent the evolution laws of physical systems. Martin et al. (1999, 2001) applied it to distinguish the time variations of electroencephalograms (EEG) in order to emphasize significant dynamic changes. Complex phenomena in the field of geophysics and environmental sciences, such as continuous seismic signals measured in volcanic areas, electromagnetic signals related with the generation of earthquakes, and time series of atmospheric particulate matter were investigated by using the FIM to get information about the dynamical mechanisms governing their time variability and to detect precursory signatures of critical phenomena (Lovallo and Telesca, 2011; Telesca and Lovallo, 2011; Telesca et al., 2010, 2011, 2009).

Shannon entropy quantifies the uncertainty of the prediction of the outcome of a probabilistic event (Shannon, 1948), being, then, zero for a deterministic event. Instead of the Shannon entropy, the so-called Shannon power entropy N_X (defined below) is generally used to avoid the difficulty of negative information measures that can arise when the Shannon entropy is used with a continuous distribution function.

Let $f(x)$ be the probability density of the SST time series, then its FIM is given by

$$\mathrm{FIM} = \int_{-\infty}^{+\infty} \left(\frac{\partial}{\partial x} f(x)\right)^2 \frac{dx}{f(x)}, \tag{1}$$

and its Shannon entropy is defined as (Shannon, 1948):

$$H_X = -\int_{-\infty}^{+\infty} f_X(x) \log f_X(x)\, dx. \tag{2}$$

As specified above, the notion of Shannon entropy power will be used (Angulo et al., 2008)

$$N_X = \frac{1}{2\pi e} e^{2H_X}. \tag{3}$$

The quantitative value of the FIM and the Shannon entropy power depends on the right computation of the probability density function $f(x)$, estimation of which can be performed by using the kernel density estimator technique (Devroye, 1987; Janicki and Weron, 1994) as shown in Eq. (4)

$$\hat{f}_M(x) = \frac{1}{Mb} \sum_{i=1}^{M} K\left(\frac{x - x_i}{b}\right), \tag{4}$$

with b the bandwidth, M the number of data and $K(u)$ the kernel function, which is a continuous non-negative and symmetric function satisfying the two following conditions

$$K(u) \geq 0 \quad \text{and} \quad \int_{-\infty}^{+\infty} K(u)\, du = 1. \tag{5}$$

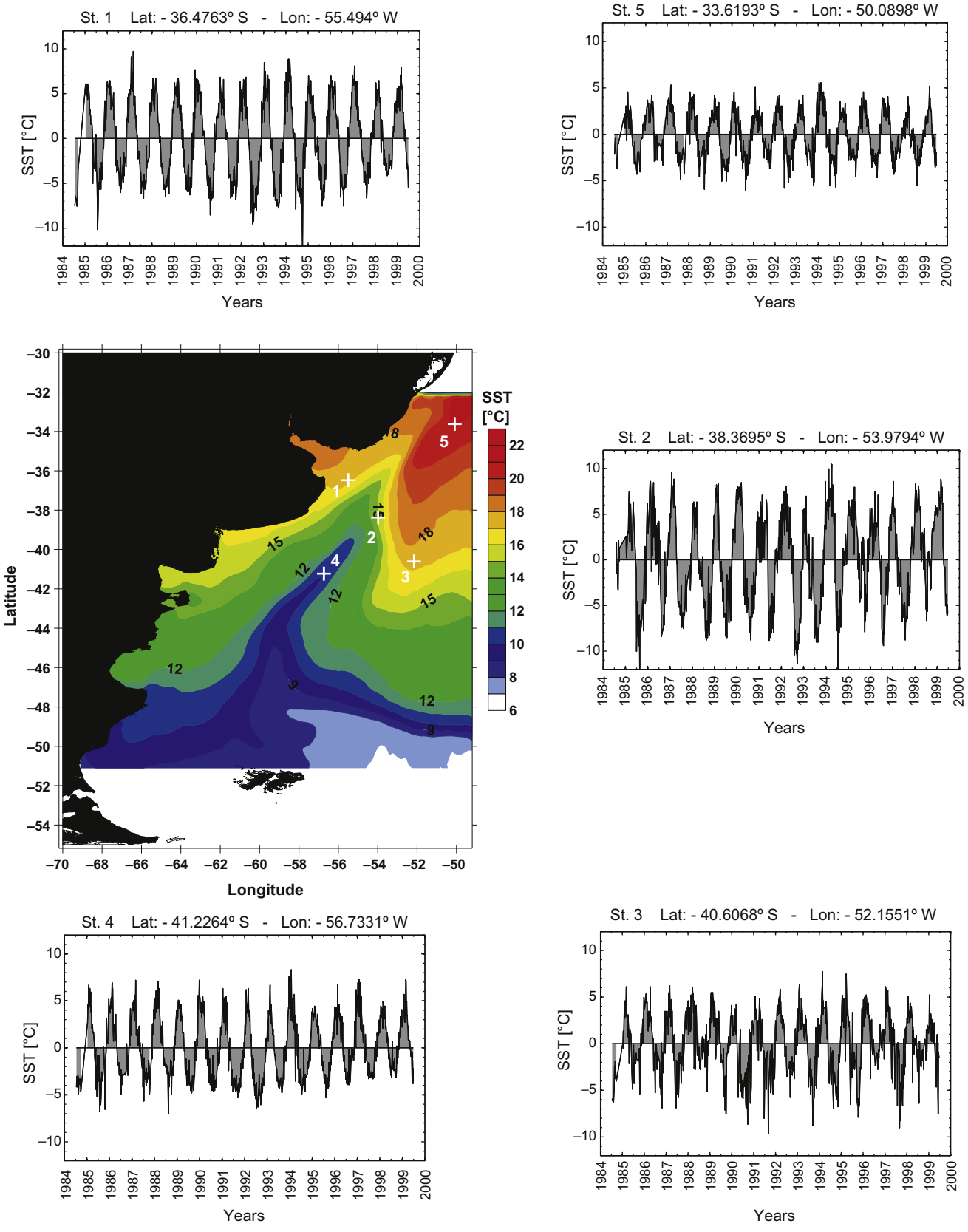

Figure 2 Spatial distribution of the mean sea surface temperature (SST) value and, as an example, the time variation of five pixels in the Brazil Malvinas Confluence Zone (BMCZ). The SST spatial patterns clearly highlights the interactions between the warmer Brazil Current and the colder Malvinas Current.

In our study, $f(x)$ was estimated by using Troudi et al.'s algorithm (2008) combined with Raykar and Duraiswami's method (2006), in which a Gaussian kernel with zero mean and unit variance is used:

$$\hat{f}_M(x) = \frac{1}{M\sqrt{2\pi b^2}} \sum_{i=1}^{M} e^{-\frac{(x-x_i)^2}{2b^2}}. \quad (6)$$

4. Results and discussion

The strong contrast in sea-surface temperature over the southwest Atlantic makes satellite infrared and color images particularly appropriate tools for studying the BMCZ. We examined 15 years (1984–1999) of AVHRR images to analyze the structure of the collision region (i.e., between 52.5°W and 56°W and 36°S and 40°S) where the Malvinas and Brazil currents produce a very active front.

Because of the presence of some anomalous SST values, very probably due to errors, a data pre-processing was performed and all the SST values deviating from the mean of more than 3 standard deviations were filtered out.

As shown in Fig. 2, the pixel time variation is subjected to seasonal cycles that are necessary to be removed before applying the FS method and to avoid any cycle-induced effect on the results. Since the sampling time of the SST data is not always regular, the cycles were not removed by using the Fourier filtering, but calculating for each 5-day composite the anomaly $SST_d = (SST - \langle SST \rangle)$ where the composite mean $\langle SST \rangle$ is calculated for each calendar day, e.g., 1st January, by averaging over all years in the record. This filtering procedure for satellite data was already applied by Telesca and Lasaponara (2005, 2006). Fig. 3 shows the spatial distribution of the mean SST_d; as it can be clearly seen, the mean SST_d is very low and homogeneously spatially distributed in the investigated area. This indicates that the filtering procedure was correctly done and the time dynamics of each pixel is not influenced by any bias due to persistent relatively high or low mean value. To each SST_d time series the FS method was applied. Figs. 4 and 5 show the spatial distribution of the FIM and Shannon entropy, respectively.

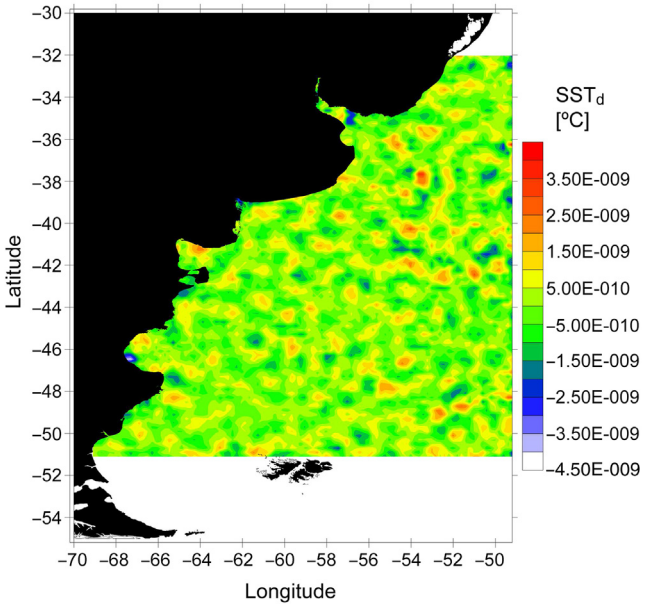

Figure 3 Spatial distribution of the mean sea surface temperature anomaly (SST_d). The mean SST_d is very low and homogeneously spatially distributed in the investigated area, indicating that the time dynamics of each pixel is not influenced by any bias due to persistent relatively high or low mean value.

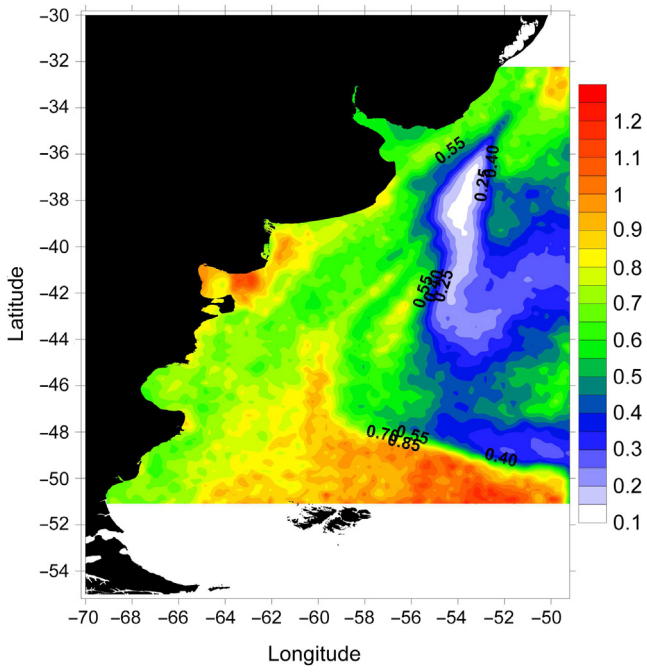

Figure 4 Spatial distribution of the Fisher information measure (FIM) of the SST_d. The BMCZ occupies the region with lower FIM.

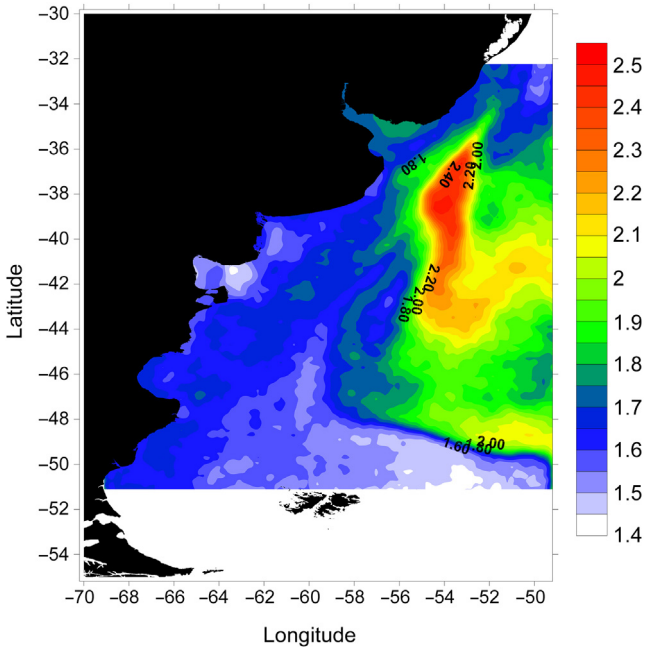

Figure 5 Spatial distribution of the Shannon entropy power of the sea surface temperature anomaly (SST_d). The BMCZ occupies the region with higher Shannon entropy.

The FIM and Shannon entropy values can be used to classify the water masses at each pixel. What is striking here, is that the FS analysis suggests that the order/organization structure of the time series of the pixels within the zone occupied by the Brazil Current and of those occupied by the Malvinas Current is rather the same. For instance, comparing the pixels, at longitude −53.4°W and varying the latitude, both the Shannon entropy (Fig. 6) and FIM (Fig. 7) show that the pixels at latitudes from −32°S and −36°S (where the Brazil Current flows) and those between −50°S and −52°S (where the Malvinas Current flows) are characterized by the same order/organization structures, being featured by high FIM and low Shannon entropy values. The same two sets of pixels, instead, are characterized by very different SST patterns, being the first set warmer than the second set (Fig. 8). It is clearly visible that the confluence occupies the region with higher Shannon entropy (Fig. 5) and lower FIM (Fig. 4) (as it can also be observed looking at the latitudinal variation of the FIM and Shannon entropy

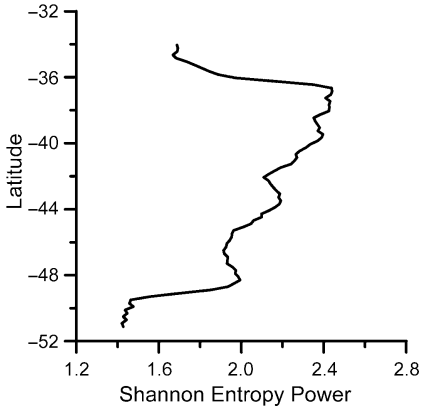

Figure 6 Profile of the Shannon entropy power at longitude 53.4°W and varying the latitude. The Shannon entropy shows that the pixels at latitudes from −32°S and −36°S (where the Brazil Current flows) and those between −50°S and −52°S (where the Malvinas Current flows) are characterized by the same order structure, being featured by high low Shannon entropy values.

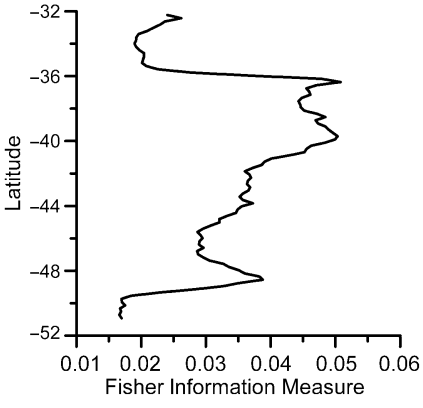

Figure 7 Profile of the Fisher information measure (FIM) at longitude 53.4°W and varying the latitude. The FIM shows that the pixels at latitudes from −32°S and −36°S (where the Brazil Current flows) and those between −50°S and −52°S (where the Malvinas Current flows) are characterized by the same organization structures, being featured by high FIM values.

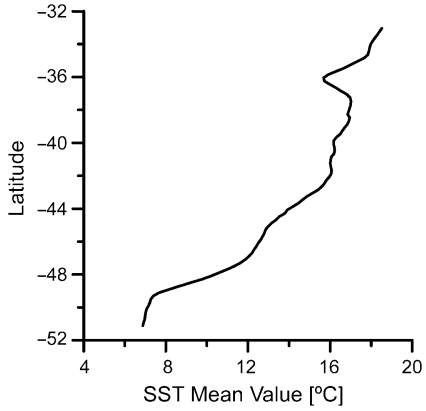

Figure 8 Profile of the SST mean value at 53.4°W and varying the latitude. The SST profile increases as the latitude increases.

(Figs. 6 and 7)); therefore, the FS analysis of the spatial distribution of the SST_d reveals that the BMCZ can be quite precisely spatially located, because it is characterized by higher Shannon entropy and lower FIM.

These results point out to a peculiar dynamical characterization of the investigated area: the warmer water masses of the Brazil Current and the colder water masses of the Malvinas Current are dynamically similar in terms of order/organization structure of the time series of the SST; while, in the BMCZ, where the two currents converge, the level of disorder (organization) of the structure of the SST time series increases (decreases). Such increase of the level of disorder is associated with a higher uncertainty and higher irregularity of the time series of the pixels occupying the BMCZ. Since the FIM and Shannon entropy have the capability to discriminate between regular and chaotic trajectories (Martin et al., 2001), the higher value of the Shannon entropy or lower value of FIM in the BMCZ indicates the higher chaotic regime that governs the dynamics of SST in the BMCZ.

This result is in agreement with the findings of Morel et al. (2014), who applied to the BMCZ an analysis of specific Lagrangian patterns in an unsteady chaotic flow which organize the transport through the regional oceanic dynamic features. The spatial distribution of their finite-time Lyapunov exponent (FTLE) shows that the high-valued zone, which corresponds to a high-mixing and high-variability zone, coincides with the BMCZ. Even the spatial distribution of the largest finite-time Lyapunov exponent (L-FTLE), estimated by computing from the geostrophic velocities, shows that the most intense values are over the BMCZ, whose dynamics is associated to stirring processes that, in general, create filaments, which are stretched in progressively thinner structures and are eventually dispersed by small-scale turbulence.

We performed a complementary analysis on the SST_d time series calculating the mean SST_d gradient distribution. For each pixel, at a specified time, the gradient magnitude is calculated using centered differences as (Saraceno et al., 2004):

$$\|grad(SST_d(i))\| = \sqrt{\left(\frac{SST_d(ix+1)-SST_d(ix-1)}{dist(ix+1,ix-1)}\right)^2 + \left(\frac{SST_d(iy+1)-SST_d(iy-1)}{dist(iy+1,iy-1)}\right)^2}, \quad (7)$$

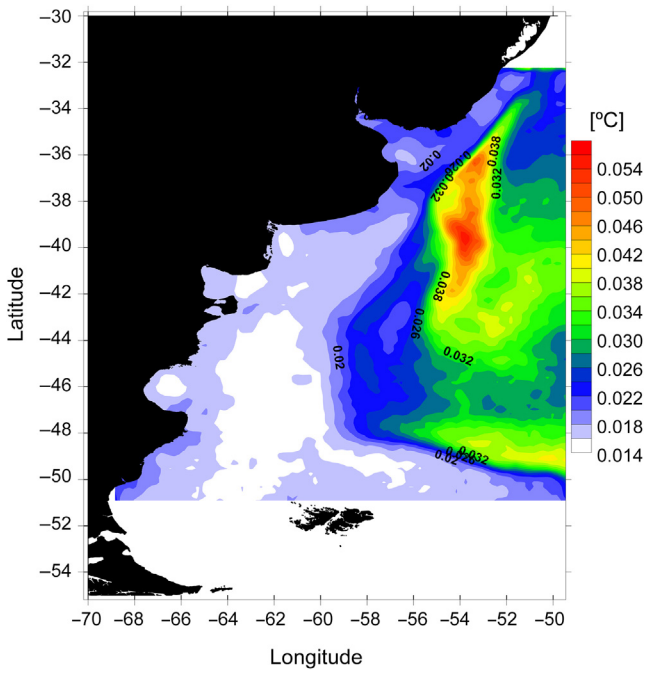

Figure 9 Spatial distribution of the gradient of the sea surface temperature anomaly (SST_d). Between 36°S and 40°S (respectively, the northern and southern limits of the Brazil-Malvinas Collision front), the mean SST_d gradient is characterized by the highest values correlating well with the Shannon entropy and FIM.

where ($ix - 1$) and ($ix + 1$) are the neighbors of the ith pixel in the X (analogously in Y) direction; *dist* is the distance in the X (analogously in Y) direction. Then, the time average of all the gradients for each pixel is calculated and the mean SST_d gradient distribution is shown in Fig. 9. Alike the Shannon entropy (Fig. 5) (FIM (Fig. 4)) on the along-shelf section shows local maxima (minima), between 36°S and 40°S (which respectively correspond to the northern and southern limits of the Brazil-Malvinas Collision front), even the mean SST_d gradient presents the highest values between these limits (Fig. 9), and, thus, it correlates well with the Shannon entropy and FIM. The mean SST (Fig. 2) shows that the transition region from the colder subantarctic waters (8–12°C) to the warmer subtropical waters (>16°C) occurs within this zone. The inflection point in Fig. 2 is located near to 38.2°S, corresponding also to the latitude of the maximum in the mean SST_d gradient. Thus we associate this point (between 52.5°W and 56°W and 36°S and 40°S) to the time-averaged position of the Brazil-Malvinas Collision front along the section. The intersection between the along-shelf section and the coincident mean positions of the Subantarctic Front and Brazil Current Front as estimated by Saraceno et al. (2004) is in good agreement with our results. In fact, the mean SST_d gradient at the along-shelf section assumes the highest values within a range of about 500 km between 38.2°S and 40°S (Fig. 6). This range of migration coincides with separation between the frontal positions derived from SST frontal probability maps obtained by Saraceno et al. (2006, 2004).

The displacement of the front along the section is also observed between the same range of latitudes for the rest of the available Shannon entropy data and for the remote sensing SST_d gradient data set.

5. Conclusions

The upper layers in the western Argentine Basin present intense current systems, such as the Brazil Current and the Malvinas Current, which are associated with strong thermocline fronts (Saraceno et al., 2004). Cross frontal mixing creates small-scale thermohaline structures (Bianchi et al., 1993, 2002), which may enhance the vertical stratification of subantarctic waters, and also lead to small-scale SST exchange (Brandini et al., 2000). In addition, current instabilities generate one of the most energetic regions of the world oceans due to the strong presence of eddies and meanders (Chelton et al., 1990). Such region is known as the Brazil–Malvinas Confluence Zone (BMCZ). For the first time, up to our knowledge, the SST time series derived from the AVHRR satellite imagery, were analyzed by using an advanced statistical method, the Fisher–Shannon method, which is capable of capturing the organizational features of a dynamical system. The calculation of the Fisher information measure (FIM) and the Shannon entropy power for all the pixel time series of SST covering the continental shelf has revealed that the most disordered and less organized structures in SST are located in correspondence with the BMCZ. This result is in good agreement with the most recent findings of chaotic behavior detected in the BMCZ.

Acknowledgements

We are grateful to PhD Guillermo Podesta (Univ. of Miami). The data set of sea surface temperature (SST) fields were derived from NOAA Advanced Very High Resolution Radiometer.

References

Anding, D., Kauth, R., 1970. Estimation of sea surface temperature from space. Rem. Sens. Environ. 1, 217–220.

Angulo, J.C., Antolin, J., Sen, K.D., 2008. Fisher–Shannon plane and statistical complexity of atoms. Phys. Lett. A 372 (5), 670–674.

Bava, J., 2004. Metodologías de procesamiento de imágenes NOAA-AVHRR y su utilización en aplica ciones oceanográficas y biológico-pesqueras en el Atlántico Sudoccidental. (Ph.D. thesis). Univ. Buenos Aires, 142 pp.

Bava, J., Gagliardini, D.A., Dogliotti, A.I., Lasta, C.A., 2002. Annual distribution and variability of remotely sensed sea surface temperature fronts in the southwestern Atlantic Ocean. In: 29th International Symposium on Remote Sensing of the Environment, Int. Soc. Rem. Sens. Environ., Buenos Aires, 8–12.

Bernstein, R.L., Chelton, D.B., 1985. Large-scale sea surface temperature variability from satellite and shipboard measurements. J. Geophys. Res. 90 (11), 619–630.

Bianchi, A.A., Giulivi, C.F., Piola, A.R., 1993. Mixing in the Brazil–Malvinas Confluence. Deep-Sea Res. Pt. I 40 (7), 1345–1358.

Bianchi, A.A., Piola, A.R., Collino, G.J., 2002. Evidence of double diffusion in the Brazil–Malvinas Confluence. Deep-Sea Res. Pt. I 49 (1), 41–52.

Blanke, B., Arhan, M., Modec, G., Rocheet, S., 1999. Warm water paths in the equatorial Atlantic as diagnosed with a general circulation model. J. Phys. Oceanogr. 29 (11), 2453–2768.

Brandini, F.P., Boltovskoy, D., Piola, A., Kocmur, S., Rottgers, R., Cesar Abreu, P., Mendes Lopes, R., 2000. Multiannual trends in fronts and distribution of nutrients and chlorophyll in the southwestern Atlantic (30—62°S). Deep-Sea Res. Pt. I 47 (6), 1015—1033.

Brown, M.G., Smith, K.B., 1990. Are SOFAR float trajectories chaotic? J. Phys. Oceanogr. 20 (1), 139—149.

Brown, M.G., Smith, K.B., 1991. Ocean stirring and chaotic low-order dynamics. Phys. Fluids 3, 1186—1192.

Chelton, D.B., Schlax, M.G., Witter, D.L., Richman, J.G., 1990. GEOSAT altimeter observations of the surface circulation of the Southern Ocean. J. Geophys. Res. 95 (C10), 17877—17903.

Denman, K.L., Abbott, M.A., 1994. Time scales of pattern evolution from cross-spectrum analysis of advanced very high resolution radiometer and coastal zone color scanner imagery. J. Geophys. Res. 99 (C4), 7433—7442.

Devroye, L.A., 1987. Course on Density Estimation. Birkhauser, Boston, 183 pp.

Doney, S., Glover, D.M., McCue, S.J., Fuentes, M., 2003. Mesoscale variability of SeaWiFS satellite ocean color: global patterns and spatial scales. J. Geophys. Res. 108 (C2), 1—15.

Evans, D.L., Signorini, S.S., Miranda, L.B., 1983. A note on the transport of the Brazil Current. J. Phys. Oceanogr. 23 (13), 1732—1738.

Fisher, R.A., 1925. Theory of statistical estimation. Proc. Camb. Philos. Soc. 22, 700—725.

Frieden, B.R., 1990. Fisher information, disorder, and the equilibrium distributions of physics. Phys. Rev. A 41 (8), 4265—4276.

Fu, L.L., 1996. The circulation and its variability of the South Atlantic Ocean: first results from the TOPEX/POSEIDON mission. In: Wefer, G., Berger, W.H., Siedler, G., Webb, D.J. (Eds.), The South Atlantic: Present and Past Circulation, Springer-Verlag, Berlin, 63—82, 644 pp.

Gordon, A.L., 1989. Brazil—Malvinas Confluence — 1984. Deep-Sea Res. Pt. I 36 (3), 359—384.

Isern-Fontanet, J., Turiel, A., Garcia-Ladona, E., Font, J., 2007. Microcanonical multifractal formalism: application to the estimation of ocean surface velocities. J. Geophys. Res. 112 (C5), C05024, 18 pp.

Janicki, A., Weron, A., 1994. Simulation and Chaotic Behavior of Alpha-Stable Stochastic Processes. Marcel Dekker, New York, 57 pp.

Kilpatrick, K.A., Podestà, G.P., Evans, R., 2001. Overview of the NOAA/NASA Advanced Very High Resolution Radiometer Pathfinder algorithm for sea surface temperature and associated matchup database. J. Geophys. Res. 106 (C5), 9179—9197.

Kushnir, Y., Robinson, W.A., Bladé, I., Hall, N.M.J., Peng, S., Sutton, R., 2002. Atmospheric GCM response to extratropical SST anomalies: synthesis and evaluation. J. Climate 15 (16), 2233—2256.

Legeckis, R., 1978. A survey of worldwide sea surface temperature fronts detected by environmental satellites. J. Geophys. Res. 83 (C9), 4501—4522.

Lentini, C., Olson, D., Podesta, G., 2002. Statistics of Brazil of current rings observed from AVHRR: 1993 to 1998. Geophys. Res. Lett. 29 (16), 1811—1814.

Lentini, C.A.D., Podestá, G.P., Campos, E.J.D., Olson, D.B., 2001. Sea surface temperature anomalies on the western South Atlantic from 1982 to 1994. Continent. Shelf Res. 21 (1), 89—112.

Lovallo, M., Telesca, L., 2011. Complexity measures and information planes of X-ray astrophysical sources. J. Stat. Mech. Theory Exp. P03029.

Maamaatuaiahutapu, K., Garçon, V., Provost, C., Mercier, H., 1998. Transports of the Brazil and Malvinas Currents at their Confluence. J. Mar. Res. 56 (2), 417—438.

Martin, M.T., Pennini, F., Plastino, A., 1999. Fisher's information and the analysis of complex signals. Phys. Lett. A 256 (2—3), 173—180.

Martin, M.T., Perez, J., Plastino, A., 2001. Fisher information and nonlinear dynamics. Physica A 291 (1—4), 523—532.

Matano, R.P., 1993. On the separation of the Brazil current from the coast. J. Phys. Oceanogr. 23 (1), 79—90.

Matano, R.P., Schlax, M.G., Chelton, D.B., 1993. Seasonal variability in the South Atlantic. J. Geophys. Res. 98 (C10), 18027—18035.

McClain, C.R., Cleave, M., Feldman, G., Gregg, W., Hooker, S., Kuring, N., 1998. Science quality SeaWiFS data for global biosphere research. Sea Technol. 39 (9), 10—14.

McClain, E.P., Pichel, W.G., Walton, C.C., 1985. Comparative performance of AVHRR-based multichannel sea surface temperatures. J. Geophys. Res. 90 (C6), 11587—11601.

Memery, L., Arhan, M., Alvarez-Salgado, X.A., Messias, M.-J., Mercier, H., Castro, C.G., Rios, A.F., 2000. The water masses along the western boundary of the south and equatorial Atlantic. Prog. Oceanogr. 47 (1), 69—98.

Morel, X., Lucas, M.A., Dos Santos, F., 2014. A Lagrangian study of the Brazil—Malvinas confluence: Lagrangian coherent structures and several Lyapunov exponents. J. Oper. Oceanogr. 7 (2), 13—23.

Njoku, E.G., 1985. Satellite-derived sea surface temperature: workshop comparisons. Bull. Am. Meteorol. Soc. 66 (3), 274—281.

Njoku, E.G., Barnett, T.P., Laurs, R.M., Vastano, A.C., 1985. Advances in satellite sea surface temperature measurement and oceanographic applications. J. Geophys. Res. 90 (C6), 573—586.

Olson, D.B., Podesta, G.P., Evans, R.H., Brown, O.B., 1988. Temporal variations in the separation of Brazil and Malvinas currents. Deep Sea Res. 35 (12), 1971—1990.

Osborne, A.R., Kirwan, A.D., Provenzale, A., Bergamasco, L., 1986. A search for chaotic behavior in large and mesoscale motions in the Pacific Ocean. Physica D 23 (1—3), 75—83.

Peterson, R.G., Stramma, L., 1990. Upper-level circulation in the South Atlantic Ocean. Prog. Oceanogr. 26 (1), 1—73.

Podesta, G.P., Brown, O.B., Evans, R.H., 1991. The annual cycle of satellite-derived sea surface temperature in the southwestern Atlantic Ocean. J. Climate 4 (4), 457—467.

Provost, C., Le Traon, P.Y., 1993. Spatial and temporal scales in altimetric variability in the Brazil—Malvinas Current Confluence region: dominance of the semiannual period and large spatial scales. J. Geophys. Res. 98 (C10), 18037—18051.

Raykar, V.C., Duraiswami, R., 2006. Fast optimal bandwidth selection for kernel density estimation. In: Proceedings of the Sixth SIAM International Conference on Data Mining, Bethesda, April 2006, 524—528.

Saraceno, M., Provost, C., Lebbah, M., 2006. Biophysical regions identification using an artificial neuronal network: a case study in the South Western Atlantic. Adv. Space Res. 37 (4), 793—805.

Saraceno, M., Provost, C., Piola, A., Bava, J., Gagliardini, A., 2004. Brazil Malvinas frontal system as seen from 9 years of advanced very high resolution radiometer data. J. Geophys. Res. 109 (5), C05027, http://dx.doi.org/10.1029/2003JC002127.

Shannon, C.E., 1948. A mathematical theory of communication. Bell Syst. Tech. J. 27, 379—423, 623—656.

Speich, S., Blanke, B., Cai, W., 2007. Atlantic meridional overturning and the Southern Hemisphere supergyre. Geophys. Res. Lett. 34 (23), L23614, http://dx.doi.org/10.1029/2007GL031583.

Stammer, D., 1997. Global characteristics of ocean variability estimated from regional TOPEX/POSEIDON altimeter measurements. J. Phys. Oceanogr. 27 (8), 1743—1769.

Telesca, L., Lasaponara, R., 2005. Discriminating dynamical patterns in burned and unburned vegetational covers by using SPOT-VGT NDVI data. Geophys. Res. Lett. 32 (21), L21401, http://dx.doi.org/10.1029/2005GL024391.

Telesca, L., Lasaponara, R., 2006. Pre- and post-fire behavioral trends revealed in satellite NDVI time series. Geophys. Res. Lett. 33 (14), L14401, http://dx.doi.org/10.1029/2006GL026630.

Telesca, L., Lovallo, M., 2011. Analysis of the time dynamics in wind records by means of multifractal detrended fluctuation analysis and the Fisher—Shannon information plane. J. Stat. Mech. P07001, 31 pp.

Telesca, L., Lovallo, M., Carniel, R., 2010. Time-dependent Fisher information measure of volcanic tremor before 5 April 2003 paroxysm at Stromboli volcano, Italy. J. Volcanol. Geotherm. Res. 195 (1), 78—82.

Telesca, L., Lovallo, M., Hsu, H.-L., Chen, C.-C., 2011. Analysis of dynamics in magnetotelluric data by using the Fisher—Shannon method. Physica A 390 (7), 1350—1355.

Telesca, L., Lovallo, M., Ramirez-Rojas, A., Angulo-Brown, F., 2009. A nonlinear strategy to reveal seismic precursory signatures in earthquake-related self-potential signals. Physica A 388 (10), 2036—2040.

Tokinaga, H., Tanimoto, Y., Xie, S.P., 2005. SST-induced surface wind variations over the Brazil—Malvinas Confluence: satellite and in situ observations. J. Climate 18 (17), 3470—3482.

Troudi, M., Alimi, A.M., Saoudi, S., 2008. Analytical plug-in method for kernel density estimator applied to genetic neutrality study. EURASIP J. Adv. Signal Process. 2008 Article ID 739082, 8 pp.

Turiel, A., Isern-Fontanet, J., García-Ladona, E., Font, J., 2005. Multifractal method for the instantaneous evaluation of the stream function in geophysical flows. Phys. Rev. Lett. 95 (10), 104502.

Vigan, X., Provost, C., Podesta, G., 2000. Sea surface velocities from sea surface temperature image sequences 2. Application to the Brazil—Malvinas Confluence area. J. Geophys. Res. 105 (C8), 19515—19534.

Vivier, F., Provost, C., 1999. Volume transport of the Malvinas Current: can the flow be monitored by TOPEX/POSEIDON. J. Geophys. Res. 104 (C9), 21105—21122.

Wainer, I., Gent, P., Goni, G., 2000. Annual cycle of the Brazil Malvinas Confluence region in the National Center for Atmospheric Research climate system model. J. Geophys. Res. 105 (C11), 167—177.